SUPPORTING INFORMATION:

Conversion of Bi-Sn Complex to Bi Nanoparticles for the Catalysis of V(II)/V(III) Kinetics

Abhinandh Sankar[†,a], Kapila Gunasekera[‡,b], Zhipeng Nan[†,c], Aaron Welton[‡], Junchuan Fang[†], Kevin Tonnis[†], Rickey Terrell[†], Punit Boolchand[‡], and Anastasios P. Angelopoulos[*,†]

[†]Department of Chemical and Environmental Engineering, University of Cincinnati, Cincinnati, OH 45221, USA.

[‡]Department of Electrical and Computer Engineering, University of Cincinnati, Cincinnati, OH 45221, USA.

Present Addresses: [a]Interplastic, OH, [b]IM Flash, Lehi, UT, [c]Storagenergy Technologies, UT

[*]Corresponding Author: angeloas@ucmail.uc.edu

Figure S1: ^{119}Sn Mössbauer Spectroscopy of the synthesis suspension at various time intervals: (a) 0 minutes, (b) 60 minutes, (c) 12 hours, (d) 24 hours, (e) 48 hours, (f) 3 days, (g) 5 days, (h) 13 days. The solid black line indicates the measured spectra while the deconvoluted spectra for the various Sn moieties are shown in color: blue for moiety A, green for moiety C, and red for moiety B, as identified in Figure 2 of the article.

Figure S2: XANES BiL_2 spectra of synthesis suspension in red at various times as indicated: time 0 (dashed line), 1 hour (dotted line), 14 days (solid line). Reference powder spectra are in black as indicated: Bi_2O_3 (dashed line), $BiCl_3$ (dotted line), Bi metal (solid line).

Figure S3: XRD pattern of BiNP in Figure 4 (c). Peak assignments are shown according to the rhombohedral structure of Bi metal. The asterix indicate the positions of much smaller BiO_x peaks while the squares indicate peaks associated with the aluminum holder.

Figure S4: (a) Magnified SEM image of a typical Bi cluster observed with 4 layers. (b) Magnified SEM image of a white cluster formed on the 20 layer sample in Figure 5(d). The cluster area contains more than 6 times the amount of Bi as the intersticial space (as determined using EDS).

Figure S5: EDS k-ratio for Bi ($I_{coating}/I_{Bi\ metal}$) with respect to the number of deposited layers.

Figure S6: X-ray photoelectron spectrum of the C1s binding energy regionfor the dried GNP (solid) and mixed BiNP-GNP (dashed) suspensions. Counts for each curve are normalized to the most prominent adventitious (C-C) carbon peak at 284.8 eV. A secondary peak appears at ~289 eV indicating the presence of an oxidized surface species (C-O).

Figure S7: (a) SEM image showing an 8 LbL layer deposit of BiNP on GC recorded at 1000x magnification. **(**b) Magnified SEM image of typical Bi clusters.

Figure S8: X-ray photoelectron spectrum of the Bi_4F binding energy region of the BiNP assembly. No metallic Bi is observed.

Figure S9: LSV showing the impact of repeated potential sweeps in 0.5 M H_2SO_4 on Bi peak intensity for a 4 layer mixed BiNP-GNP assembly (a) when no NaOH wash is employed (the inset expands the potential region where Sn removal occurs) and (b) after 1 min wash in 0.25 M NaOH. Scan rate of 50 mV s^{-1}.

Figure S10. The initial, 50^{th}, and 100^{th} consecutive CV's of 8 layers of BiNP-GNP deposited on a GC electrode in 2 M H_2SO_4. The sweep rate was 20 mV s^{-1}.

Figure S11. LSV in the Bi stripping region of the samples subjected to CV cycling as in Figure S6. Normalized current density depicts relative loss in Bi content.

Figure S12: LSV showing the impact of repeated potential sweeps in 0.5 M H_2SO_4 on Bi peak intensity for an 8 layer BiNP assembly after 1 min wash in 0.25 M NaOH. Scan rate of 50 mV s^{-1}.

Figure S13: RDE voltammograms of (a) 4, 8, and 20 layer assemblies of mixed BiNP-GNP at 750 rpm in N_2-saturated 0.1M V(III) + 2M H_2SO_4 solution, (b) 8 assembled layers of pure GNP at different rotation speeds ranging from 200 rpm to 2000 rpm in 0.1M V(III) + 2M H_2SO_4 electrolyte conditions, and (c) as in (b) but utilizing 8 assembled layers of mixed BiNP-GNP. Inset plot in (c) illustrates Levich behavior.

Figure S14: (a) Koutecky-Levich plots obtained from hydrodynamic voltammograms for 4,8, and 20 layers of mixed BiNP-GNP at -0.70 V (vs Ag/AgCl), (b) comparison of K-L analysis for 8 assembled layers with Bi (at -0.70 V vs. Ag/AgCl) and without Bi (at -0.85 V vs Ag/AgCl), as labeled, and (c) K-L plots of 8 layers of mixed BiNP-GNP obtained at different potentials. All in in N_2-saturated 0.1M V(III) + 2M H_2SO_4 solution.

Table S1: Elemental Data of BiNP from EDS

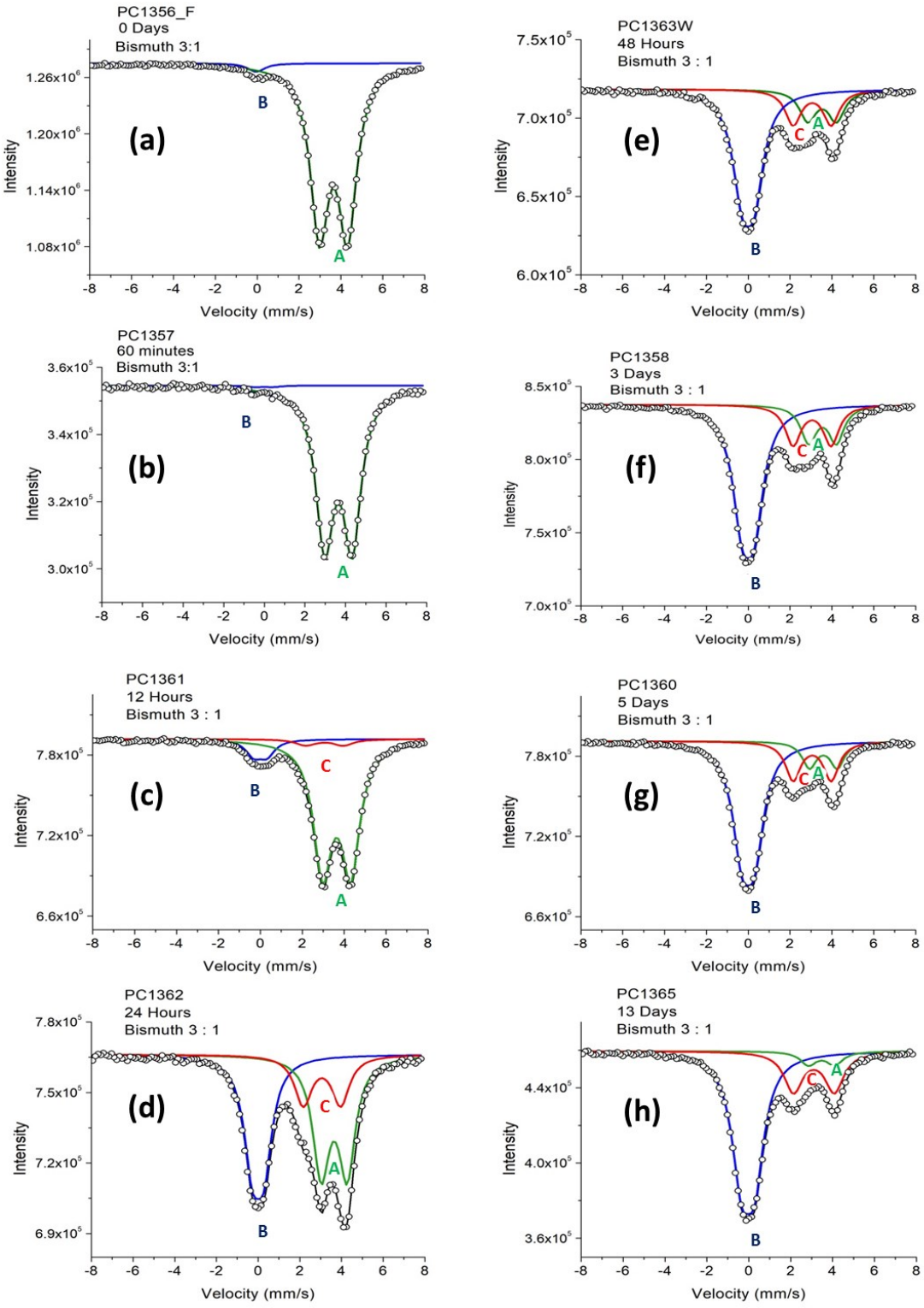

Figure S1. ^{119}Sn Mössbauer Spectroscopy of the synthesis suspension at various time intervals: (a) 0 minutes, (b) 60 minutes, (c) 12 hours, (d) 24 hours, (e) 48 hours, (f) 3 days, (g) 5 days, (h) 13 days. The solid black line indicates the measured spectra while the deconvoluted spectra for the various Sn moieties are shown in color: green for moiety A, blue for moiety B, and red for moiety C, as identified in Figure 2 of the article.

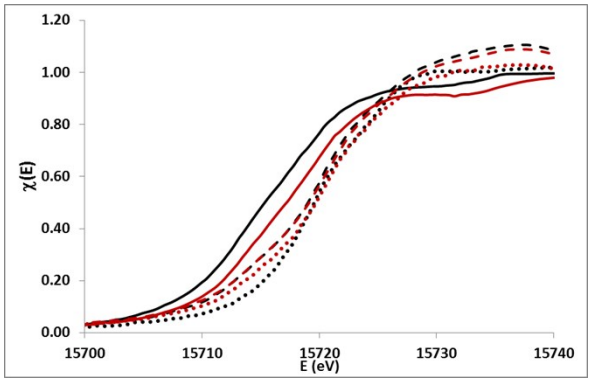

Figure S2. XANES BiL_2 spectra of synthesis suspension in red at various times as indicated: time 0 (dashed line), 1 hour (dotted line), 14 days (solid line). Reference powder spectra are in black as indicated: Bi_2O_3 (dashed line), $BiCl_3$ (dotted line), Bi metal (solid line).

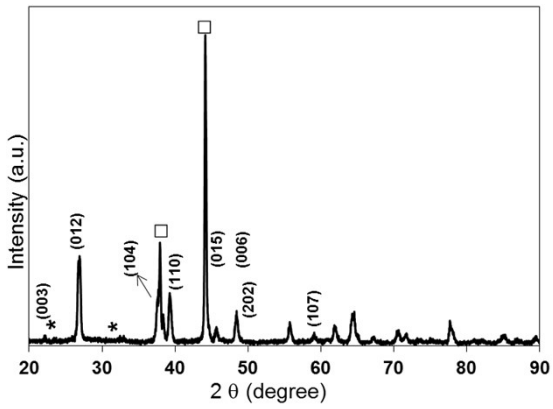

Figure S3. XRD pattern of BiNP in Figure 4 (c). Peak assignments are shown according to the rhombohedral structure of Bi metal. The asterix indicate the positions of much smaller BiO_x peaks while the squares indicate peaks associated with the aluminum holder.

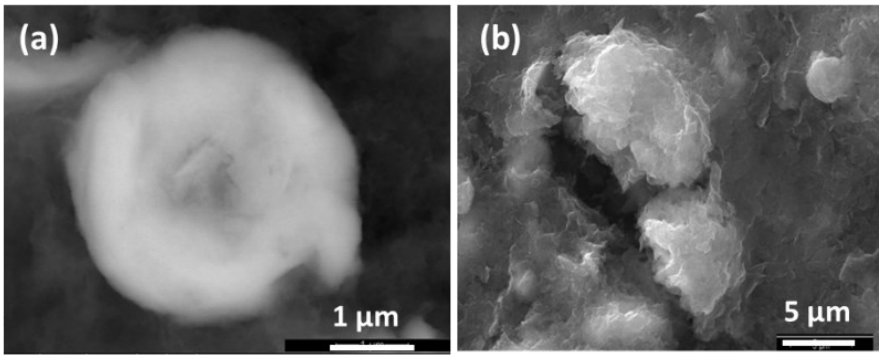

Figure S4. (a) Magnified SEM image of a typical Bi cluster observed with 4 layers. (b) Magnified SEM image of a white cluster formed on the 20 layer sample in Figure 5(d). The cluster area contains more than 6 times the amount of Bi as the intersticial space (as determined using EDS) .

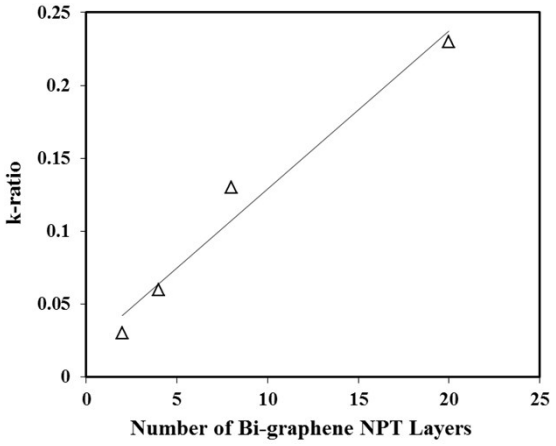

Figure S5. EDS k-ratio for Bi ($I_{coating}/I_{Bi\ metal}$) with respect to the number of deposited layers.

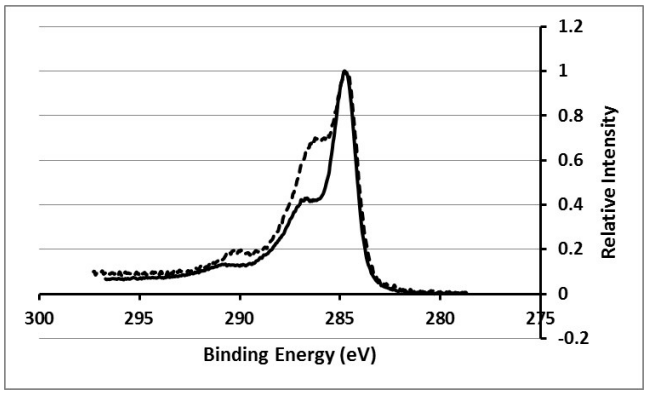

Figure S6. X-ray photoelectron spectrum of the C1s binding energy region for the dried GNP (solid) and mixed BiNP-GNP (dashed) suspensions. Counts for each curve are normalized to the most prominent adventitious (C-C) carbon peak at 284.8 eV. A secondary peak appears at ~289 eV indicating the presence of an oxidized surface species (C-O).

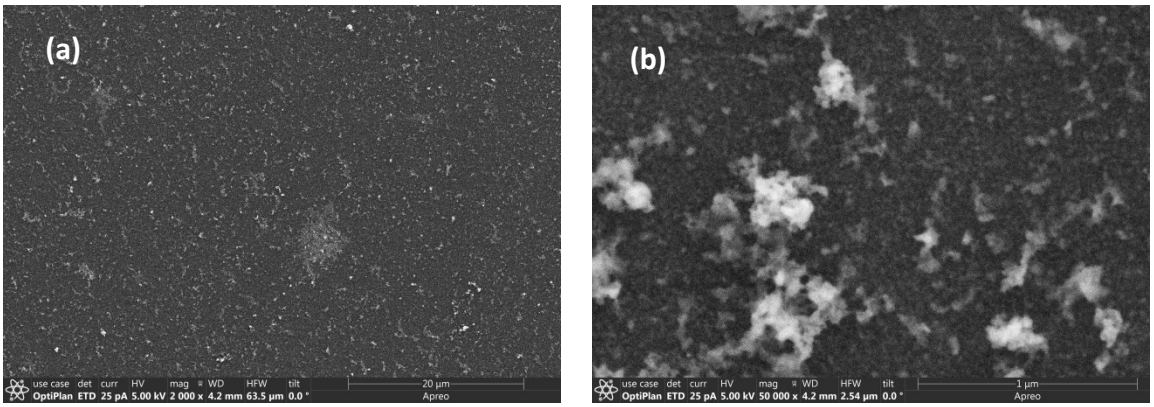

Figure S7. (a) SEM imag ded at 1000x magnification. (b) Magnified SEM imag

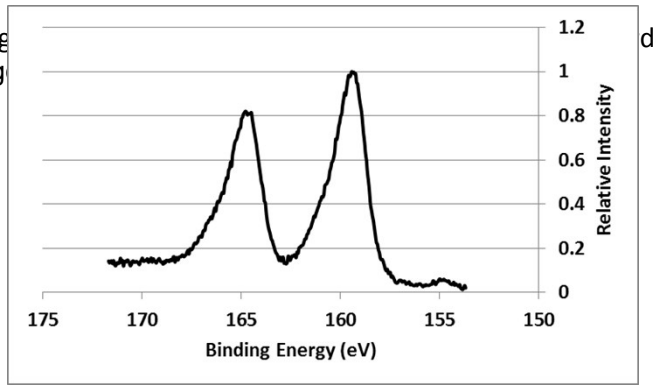

Figure S8. X-ray photoelectron spectrum of the Bi4F binding energy region of the 8 layer BiNP LbL assembly. No metallic Bi is observed.

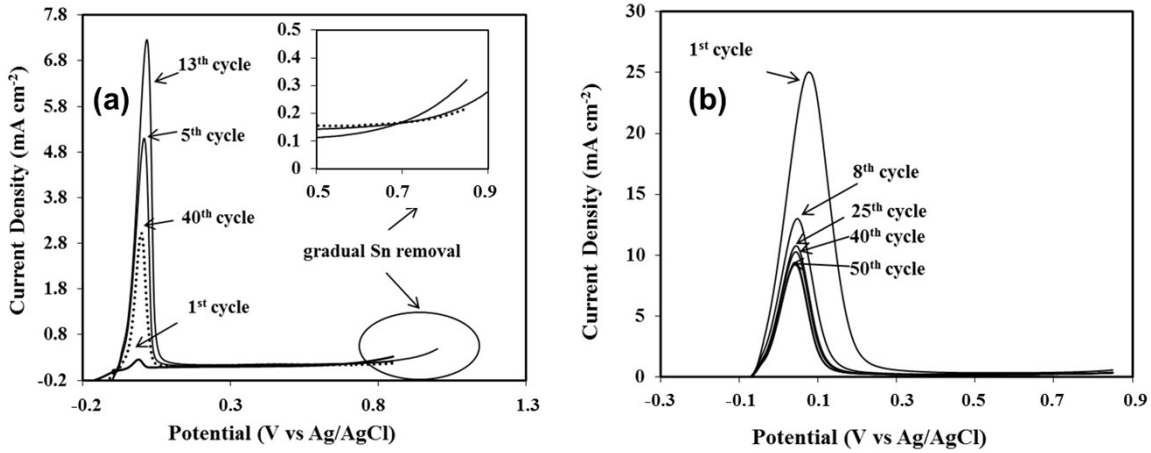

Figure S9. LSV showing the impa M H_2SO_4 on Bi peak intensity for a 4 layer mixed BiNP-GNP assem d (the inset expands the potential region where Sn remova 5 M NaOH. Scan rate of 50 mV s^{-1}.

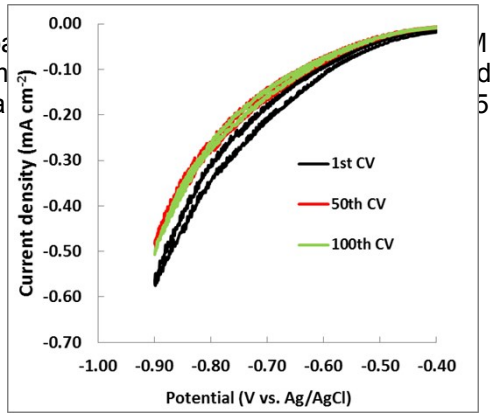

Figure S10. The initial, 50th, and 100th consecutive CV's of 8 layers of BiNP-GNP deposited on a GC electrode in 2 M H_2SO_4. The sweep rate was 20 mV/s.

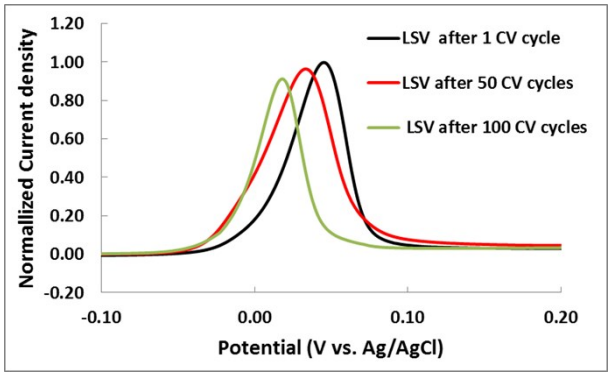

Figure S11. LSV in the Bi stripping region of the samples subjected to CV cycling as in Figure S10. Normalized current density depicts relative loss in Bi content.

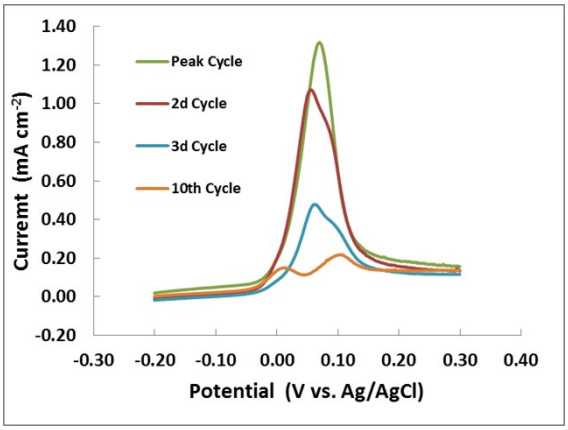

Figure S12. LSV showing the impact of repeated potential sweeps in 0.5 M H_2SO_4 on Bi peak intensity for an 8 layer BiNP assembly after 1 min wash in 0.25 M NaOH. Scan rate of 50 mV s^{-1}.

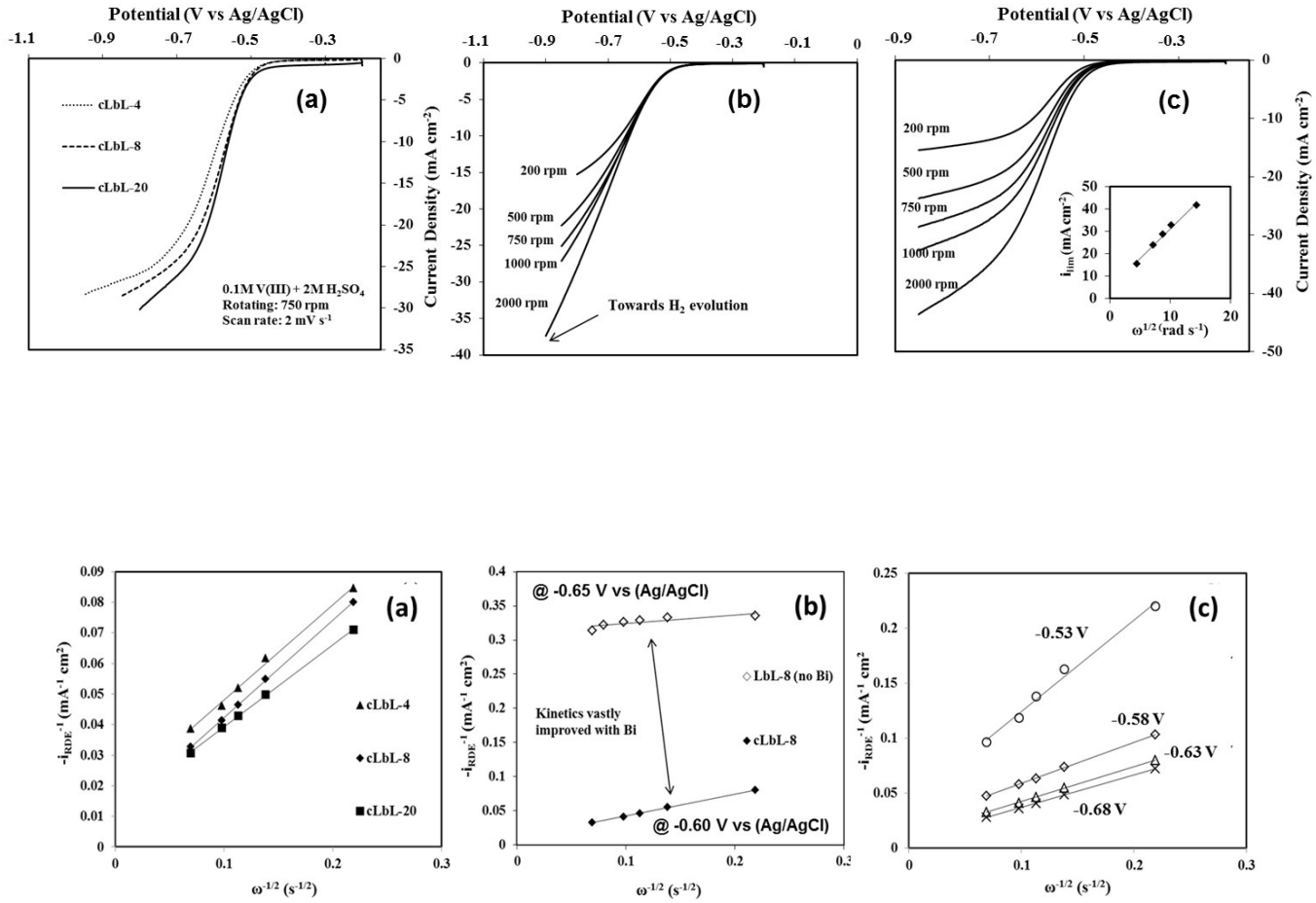

Figure S14. (a) Koutecky-Levich plots obtained from hydrodynamic voltammograms for 4,8, and 20 layers of mixed BiNP-GNP at -0.6 V (vs Ag/AgCl), (b) comparison of K-L analysis for 8 assembled layers with Bi (at -0.6 V vs. Ag/AgCl) and without Bi (at -0.65 V vs Ag/AgCl), as labeled, and (c) K-L plots of 8 layers of mixed BiNP-GNP obtained at different potentials. All in in N_2-saturated 0.1M V(III) + 2M H_2SO_4 solution.

Table S1. Elemental Data of BiNP from EDS

Sample	Weight %			
	Bi	O	Sn	Cl
water washed	41.2	6.4	43.3	9.1

7.5 M HCl immersion for 5 min.	92.3	6.2	0.2	1.3